Electronic Supplementary Information

for

Synergistic valence tautomerism and fluorescence emission in a two-dimensional coordination polymer

Wen-Ting Liu, Jie-Sheng Hu, Meng Yu,* Jin-Peng Xue, Zhi-Kun Liu, Jia-Ping Wang and Jun Tao*

Key Laboratory of Cluster Science of Ministry of Education, School of Chemistry and Chemical Engineering, Liangxiang Campus, Beijing Institute of Technology, Beijing 102488, People's Republic of China

E-mail: mengyu@bit.edu.cn, taojun@bit.edu.cn

Contents

1. Instruments and Methods

Materials and Methods. All reagents and deuterated solvents were used as purchased without further purification. NMR spectra were recorded on a Bruker Advance 300 MHz spectrometer. Thermogravimetric analyses (TGA) were carried out from 298 to 773 K on a Hitachi TG-DTA 7200 instrument with a heating rate of 2 $K\ min^{-1}$ under N_2 flow. Fourier transform infrared (FT-IR) spectra were recorded on a Bruker ALPHA FT-IR spectrometer in the range of 400−4000 cm^{-1}. Solid-state UV−vis spectra were recorded on a TU-1901 dual-beam UV−vis spectrophotometer with $BaSO_4$ as reference in the range of 280−800 nm. N_2 sorption isotherms were measured at 77 K using a Quantachrome Instrument ASiQMVH002-5 after pretreatment (samples were degassed at 80 °C for 10 h). X-band EPR spectra were recorded using a JNM-ECAE600 spectrometer. Powder X-ray diffraction (PXRD) patterns were collected on a Bruker D8 Advance (40 kV, 40 mA) diffractometer with Cu radiation (λ = 1.54184 Å) at room temperature. Simulated PXRD patterns were generated using Mercury 2021.1.0.

Single-Crystal X-ray Diffraction. SC-XRD analysis of **1** was performed on a Bruker D8 VENTURE X-ray diffractometer equipped with graphite-monochromated Cu Kα radiation (λ = 1.54178 Å). Crystallographic data of **1** were collected in a cooling N_2 stream at 180 K. Because **1** is not sufficiently stable at room temperature and cannot be collected for a long time, the room temperature (298 K) crystal data of **1** was collected with a Bruker/ARINAX MD2 diffractometer equipped with a MarCCD-300 detector (λ = 0.71073 Å) at the BL17B beam line station of the Shanghai Synchrotron Radiation Facility (SSRF).

The structures were solved by direct methods and further refined by full-matrix least-squares techniques on F^2 with SHELX program.[1] The hydrogen atom positions were fixed geometrically at calculated distances and allowed to ride on the parent atoms. Due to the instability of crystals at room temperature (298 K) and its large porous structure, attempts to define the highly disordered solvent molecules at 298 K was unsuccessful. Therefore, the structure at 298 K was refined with the PLATON "SQUEEZE" procedure.[2] CCDC 2204959-2204960 contain the supplementary crystallographic data for this paper. These data can be obtained free of charge from The Cambridge Crystallographic Data Centre via http://www.ccdc.cam.ac.uk/datarequest/cif.

Crystal data and selective bond lengths and angles are summarized in Tables S1 and S2.

Magnetic Susceptibility Measurements. Variable-temperature magnetic susceptibilities were

measured on a Quantum Design MPMS XL7 magnetometer under magnetic field of 5000 Oe at temperature range of 2−380 K with a sweeping rate of 2 $K\,min^{-1}$. The samples used for the magnetic measurements of Fig. 2 were prepared from the standard method described above and soaked in acetone, cyclohexane and *n*-butanol, respectively, for three times within two days (their relative molecular masses were determined by TGA), while that for the magnetic measurement of Supplementary Fig. S8 was prepared by heating and evacuating the sample of **1** at 353 K overnight. The prepared samples were tightly wrapped with a drop of crystal oil by a plastic film ($2 \times 2\ cm^2$) and fixed in a straw, which were loaded in the SQUID chamber at 300 K.

Computational Methods. Density functional theory (DFT) calculations were performed using the ORCA quantum chemistry software version 4.2.1.[3] Initial atomic coordinates of the simplified model complex were obtained from the crystal structure of **1** at 298 K. Then geometrical optimizations were carried out in the gas phase using B3LYP functional with a double-z basis set with polarization functions (def2-SVP) on all atoms except cobalt, for which a valence triple-z basis set (def2-TZVP) was used. The validity of structural solutions was checked by performing frequency calculations and no negative frequencies were observed. Single point energies for different spin states were calculated by OPBE, B3LYP*, and TPSSh functionals with def2-TZVP basis set applied for all the atoms. Note that both dispersion correction and relativistic effect tend to stabilize the lower spin state. The RI and RIJCOSX approximations[4] combined with appropriate auxiliary basis sets[5] were routinely employed to speed up the calculations. Grid-6 and TightSCF convergence criteria (energy: 1.0×10^{-8} au) were used for all calculations.

TD-DFT. The time-dependent DFT calculations were conducted for **1** in both HS-$Co^{II}(Sq)_2$ and LS-Co^{III}(Cat)(Sq) tautomeric forms. RIJCOSX approximation was employed to speed up the calculation. Geometries optimized with the spin-unrestricted B3LYP functional in gas phase were used for TD-DFT single-point calculation with the range separated hybrid CAM-B3LYP to take into account any possible charge transfer (CT) excitations. Calculations were done with the def2-SVP basis set on all atoms except cobalt, oxygen, and nitrogen, for which a valence triple-z basis set (def2-TZVP) was used. Calculated UV-vis spectra were obtained using orca_mapspc program with a Gaussian peak width of 2500 cm^{-1} to obtain convoluted and deconvoluted spectra, respectively, and the stick spectra show the absorption wavelengths and oscillator strengths. Orbital transitions with major contributions are reported with an isovalue of 0.05.[6]

In the B3LYP optimized structure for LS-Co^{III}(Cat)(Sq) isomer (S = 1/2), the coordinative environment around Co^{III} ion agrees quite well with the crystal structure, further corroborating the above S = 1/2 spin assignment for **1** at 298 K based on crystal data (Table S3). The relative energies of HS-$Co^{II}(Sq)_2$ (S = 5/2) and LS-Co^{III}(Cat)(Sq) (S = 1/2) electronic states were computed by the B3LYP*, OPBE, and TPSSh functionals as recent theoretical research on VT complexes revealed that these functionals correlate well with experimental observations. The calculated energies were summarized in Table S4. The B3LYP* functional predicts a close energy difference of 2.8 kcal/mol between the two energetic states, in accordance with the occurrence of VT transition at accessible temperatures. The OPBE and TPSSh functionals produce larger energy gaps between the electromers but these values fall within reasonable range for VT systems nevertheless. Note that the calculated structures are merely simplified models whereas other determining factors including intermolecular interactions in crystal lattice can have dramatic impact on the magnetic behaviors.

2. Synthetic procedures

Synthesis of 1,1,2,2-tetrakis(4-bromophenyl)ethene. 1,1,2,2-tetrakis(4-bromophenyl)ethene was synthesized by a literature method.[7]

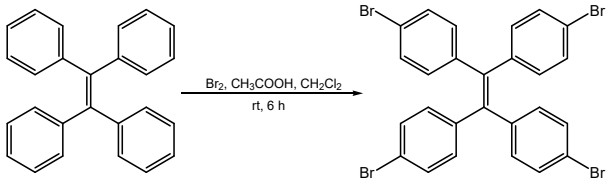

In an ice water bath, molecular bromine (38.4 g, 12.32 mL, 240 mmol) was added to the glacial acetic acid (15 ml) and dichloromethane solution (60 ml) of 1,1,2,2-tetraphenylethene (6.0 g, 30.0 mmol). The resulting mixture was then stirred at room temperature for 6 h, and poured into 400 ml ice water and then extracted three times with dichloromethane. The organic phase was washed with hydrogensulfite, water, and brine in turn, dried over $MgSO_4$, finally the solvent was removed under reduced pressure. The crude product was recrystallized with cyclohexane to give 1,1,2,2-tetrakis(4-bromophenyl)ethene (10.4 g, 16.04 mmol, 53% yield) as a colorless solid. ^{1}H NMR (400 MHz, $CDCl_3$, 298K): δ 7.20–7.31 (m, 8H), 6.76–6.91 (m, 8H).

Synthesis of 1,1,2,2-tetrakis(4-(pyridin-4-yl)phenyl)ethene (TPPE). Ligand TPPE was synthesized according to the reference method.[8]

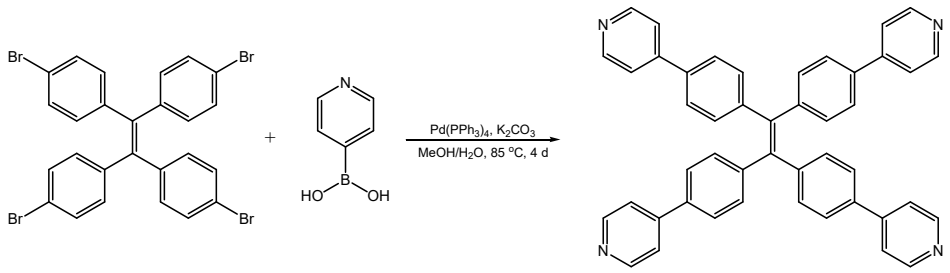

1,1,2,2-Tetrakis(4-bromophenyl)ethene (2.00 g, 3.08 mmol), 4-pyridinylboronic acid (2.28 g, 18.52 mmol), K_2CO_3 (5.12g, 18.52mmol), $Pd(PPh_3)_4$ (720 mg, 0.62 mmol) were added into a 500 mL round-bottom flask. Then toluene, methanol and water (4:1:1, 240 mL) after being injected with nitrogen were added to the round-bottom flask. The whole system was degassed and purged with nitrogen by freeze-pump-thaw for 3 times. The mixture was refluxed at 85 ℃ for 4 days. After cooling, the aqueous and organic phases were separated and then the aqueous phase was extracted with dichloromethane. Finally, the combined organic solvents of toluene and dichloromethane were removed under reduced pressure to give a crude product, which was purified by flash column chromatography (CH_2Cl_2/MeOH = 10:1) to give product TPPE (1.4 g, 71%) as a faint yellow solid. ^{1}H NMR (400 MHz, $CDCl_3$, 298K): δ 8.63 (d, J = 5.7 Hz, 8H), 7.44–7.53 (m, 16H), 7.23 (d, J = 8.3 Hz, 8H).

Synthesis of compound (1). A toluene/methanol solution (7:1, 2 mL) of TPPE (0.0064 g, 0.01 mmol) and 3,5-di-*tert*-butyl-1,2-catechol (0.0089 g, 0.04 mmol) were put in the bottom of a test tube, upon which a buffer layer of toluene/methanol (2:1, 2 mL) was added, then a methanol solution (2 mL) of $Co(OAc)_2{\cdot}4H_2O$ (0.005 g, 0.02 mmol) was carefully layered. After one week, dark green crystals were formed. The amount of solvent molecules contained in the crystal was determined on the basis of thermogravimetric and elemental analysis results (Fig. S1). Calcd for **1**·$6CH_3OH{\cdot}2C_6H_5CH_3$($C_{71}H_{96}CoN_2O_{10}$): C, 71.27; H, 8.09; N, 2.34. Found: C, 75.28; H, 6.65; N, 2.85. Guest molecules estimated from CHN analysis were not fully consistent with the theoretical value of the solvent molecules, because the sample lost partial lattice solvent molecules and absorbed water molecules in air.

3. Additional Tables

Table S1. Crystal data and structural refinements for **1**.

	1	
T / K	180	298
Formula	$C_{51}H_{56}CoN_2O_4 \cdot 2C_7H_8$[a]	$C_{51}H_{56}CoN_2O_4$
M_r / g mol^{-1}	1004.17	819.9
Crystal system	Monoclinic	
Space group	$C2/m$	
a / Å	19.087(5)	19.571(2)
b / Å	34.674(5)	34.924(4)
c / Å	12.113(2)	12.1538(12)
α / °	90	90
β / °	105.60(2)	107.312(4)
γ / °	90	90
V / Å^3	7722(3)	7930.8(15)
Z	4	
μ / mm^{-1}	2.033	0.242
F(000)	2212.0	1740.0
R_{int} / %	5.17	6.12
R_1 [$I \geq 2\sigma(I)$]	0.0643	0.1081
wR_2 (all data)	0.1964	0.2888
CCDC no.	2204959	2204960

[a]The methanol solvent molecules were unable to identify due to the partial loss during the process of picking crystals and the disorder of methanol molecules.

Table S2. Selected bond lengths and angles for **1**.

	1	
T / K	180	298
Co1-O1 / Å	1.889(2)	1.881(4)
Co1-O2 / Å	1.8856(18)	1.891(3)
Co1-N1 / Å	1.9417(19)	1.957(3)
O1-C2 / Å	1.328(3)	1.332(6)
O2-C1 / Å	1.317(3)	1.324(6)
C1-C2 / Å	1.436(4)	1.422(7)
C2-C3 / Å	1.423(4)	1.437(8)
C3-C4 / Å	1.380(4)	1.371(9)
C4-C5 / Å	1.418(5)	1.400(10)
C5-C6 / Å	1.390(4)	1.390(9)
C6-C1 / Å	1.389(4)	1.382(8)
O2^1–Co1–N1^1	89.47(8)	89.82(15)
O2^1–Co1–N1	90.54(8)	90.18(15)
O2–Co1–N1^1	90.53(8)	90.18(15)

O2–Co1–N1	89.47(8)	89.82(15)
O1[1]–Co1–O2	92.56(8)	92.96(16)
O1[1]–Co1–O2[1]	87.44(8)	87.04(16)
O1–Co1–O2[1]	92.56(8)	92.96(16)
O1–Co1–O1[1]	180.0	180.0
O1–Co1–N1[1]	89.30(8)	89.57(16)
O1–Co1–N1	90.70(8)	90.44(16)
O1[1]–Co1–N1	89.30(8)	89.56(16)
O1[1]–Co1–N1[1]	90.70(8)	90.44(16)
N1[1]–Co1–N1	180.0	180.00(12)
C1–O1–Co1	109.91(17)	110.8(3)
C2–O2–Co1	109.99(16)	109.6(3)
Σ / deg[a]	15.1889	14.3785
Θ / deg[b]	47.9707	54.4246
Diox MOS[c]	-1.45	-1.50
Cobalt BVS[d]	3.04	3.01

180 K Symmetry code: 1) – *x* + 3/2, – y + ½, – z +1 for 180 K; – *x* + 3/2, – y + 3/2, – z +1 for 298 K.

[a] The sum of the deviation of 12 unique *cis* ligand-metal-ligand angles from 90°. [b] The sum of the deviation of 24 unique torsional angles between the ligand atoms on opposite triangular faces of the octahedron viewed along the *pseudo*-threefold axis from 60°. [c] Empirical metrical oxidation state of tetraoxolene ligands, proposed by Brown et al. uses a least-squares fitting of C–C and C–O bond lengths to assign an apparent oxidation state: −1 for a semiquinonate ligand and −2 for a catecholate ligand. [d] The calculated bond valence sum (BVS).

Table S3. Selected calculated excitation energies, corresponding oscillator strengths (*f*), and assignment of the electronic transitions of LS-Co^{III}(Cat)(Sq) (*S* = 1/2) and HS-$Co^{II}(Sq)_2$ (*S* = 5/2) electronic states.

LS-Co^{III}(Cat)(Sq) (*S* = 1/2)				**HS-$Co^{II}(Sq)_2$ (*S* = 5/2)**			
Excited states	***f***	**Major contributions**	**Assignment**	**Excited states**	***f***	**Major contributions**	**Assignment**
0.371 eV/3343(?) nm	0.1611	HOMO(β) → LUMO(β) (0.93)	IVCT (Cat^{2-} → $Sq^{\bullet-}$)	2.219 eV/559 nm	0.0242	HOMO-2(β) → LUMO(β) (0.50) HOMO-3(β) → LUMO+1(β) (0.40)	$Sq^{\bullet-}$ π → π*
1.694 eV/732	0.0042	HOMO(β) → LUMO+9(β)	LMCT (Cat^{2-} → LS-Co^{III} e_g*)	3.067 eV/404	0.1198	HOMO-4(β) → LUMO(β) (0.83)	MLCT (HS-Co^{II} t_{2g} → $Sq^{\bullet-}$)

nm		(0.83)		nm			
1.904 eV/651 nm	0.0084	HOMO-2(β) → LUMO(β) (0.92)	$Sq^{\bullet-}$ π → π*	3.618 eV/372 nm	0.0024	HOMO-5(β) → LUMO(β) (0.61) HOMO-13(β) → LUMO(β) (0.16)	MLCT (HS-Co^{II} e_g* → $Sq^{\bullet-}$) IL (ML e_g orbital → $Sq^{\bullet-}$)
3.073 eV/404 nm	0.0120	HOMO-1(α) → LUMO+8(α) (0.64)	LMCT (Cat^{2-} → LS-Co^{III} e_g*)	3.618 eV/343 nm	0.0091	HOMO(α) → LUMO(α) (0.49) HOMO(α) → LUMO+2(α) (0.35)	LL'CT ($Sq^{\bullet-}$ → TPPE) LL'CT ($Sq^{\bullet-}$ → TPPE)
3.080 eV/403 nm	0.0022	HOMO(β) → LUMO+13(β) (0.59) HOMO(β) → LUMO+11(β) (0.17) HOMO(β) → LUMO+15(β) (0.11)	LL'CT (Cat^{2-} → TPPE) LL'CT (Cat^{2-} → TPPE) LL'CT (Cat^{2-} → TPPE)	3.659 eV/339 nm	0.0158	HOMO-34(β) → LUMO+1(β) (0.24) HOMO-40(β) → LUMO(β) (0.17) HOMO-34(β) → LUMO(β) (0.12)	IL (ML t_{2g} orbital → $Sq^{\bullet-}$) IL (ML t_{2g} orbital → $Sq^{\bullet-}$) IL (ML t_{2g} orbital → $Sq^{\bullet-}$)
3.090 eV/401 nm	0.0024	HOMO(α) → LUMO+11(α) (0.37) HOMO-1(α) → LUMO+8(α) (0.10) HOMO-25(β) → LUMO+12(β) (0.10)	LMCT ($Sq^{\bullet-}$ → LS-Co^{III} e_g*) LMCT (Cat^{2-} → LS-Co^{III} e_g*) LMCT(Cat^{2-} / $Sq^{\bullet-}$ → LS-Co^{III} e_g*)	3.659 eV/339 nm	0.0079	HOMO-34(β) → LUMO(β) (0.23) HOMO(β) → LUMO+1(β) (0.12) HOMO-40(β) → LUMO+1(β) (0.11) HOMO-4(β) → LUMO+1(β) (0.10)	IL (ML t_{2g} orbital → $Sq^{\bullet-}$) L'LCT (TPPE → $Sq^{\bullet-}$) IL (ML t_{2g} orbital → $Sq^{\bullet-}$) MLCT (HS-Co^{II} t_{2g} → $Sq^{\bullet-}$)

3.135 eV/396 nm	0.0019	HOMO-1(α) → LUMO+11(α) (0.80)	LMCT (Cat^{2-} → LS-Co^{III} e_g*)	3.769 eV/329 nm	0.0142	HOMO-1(α) → LUMO+1(α) (0.46) HOMO-1(α) → LUMO+3(α) (0.34)	LL'CT ($Sq^{\bullet-}$ → TPPE) LL'CT ($Sq^{\bullet-}$ → TPPE)
3.245 eV/382 nm	0.0036	HOMO(α) → LUMO(α) (0.47) HOMO(α) → LUMO+2(α) (0.32)	LL'CT ($Sq^{\bullet-}$ → TPPE) LL'CT ($Sq^{\bullet-}$ → TPPE)	3.779 eV/328 nm	1.9697	HOMO-3(α) → LUMO+1(α) (0.21) HOMO-2(α) → LUMO(α) (0.23) HOMO-1(β) → LUMO+3(β) (0.22) HOMO(β) → LUMO+2(β) (0.22)	TPPE π → π* TPPE π → π* TPPE π → π* TPPE π → π*
3.575 eV/347 nm	0.0084	HOMO-4(β) → LUMO(β) (0.94)	L'LCT (TPPE → $Sq^{\bullet-}$)	3.790 eV/327 nm	0.0084	HOMO-3(α) → LUMO(α) (0.21) HOMO-2(α) → LUMO+1(α) (0.21) HOMO-1(β) → LUMO+2(β) (0.22) HOMO(β) → LUMO+3(β) (0.21)	TPPE π → π* TPPE π → π* TPPE π → π* TPPE π → π*
3.750 eV/331 nm	2.0615	HOMO-3(α) → LUMO(α) (0.22) HOMO-2(α) →	TPPE π → π* TPPE π → π* TPPE π → π*	4.180 eV/297 nm	0.0525	HOMO-1(α) → LUMO+31(α) (0.26)	$Sq^{\bullet-}$ π → π* $Sq^{\bullet-}$ π → π*

		LUMO+1(α) (0.22) HOMO-4(β) → LUMO+1(β) (0.22) HOMO-3(β) → LUMO+2(β) (0.22)	TPPE π → π*			HOMO(α) → LUMO+33(α) (0.30)	
3.782 eV/328 nm	0.0114	HOMO(β) → LUMO+8(β) (0.44)	LL'CT (Cat^{2-} → TPPE)				

Table S4. Comparison of selected bond lengths between crystallographic data (298 K) and DFT (B3LYP) optimized structure LS-Co^{III}(Cat)(Sq).

	Calcd. / Å	Exptl. / Å
Co^{III}-N_{TPPE}	1.974, 1.974	1.957, 1.957
Co^{III}-$O_{Cat/Sq}$	1.889, 1.893	1.881,1.891
Co^{III}-$O_{Cat/Sq}$	1.890, 1.894	1.881,1.891

Table S5. Relative energies *E*(kcal/mol) for LS-Co^{III}(Cat)(Sq) (*S* = 1/2) and HS-$Co^{II}(Sq)_2$ (*S* = 5/2) electronic states obtained from DFT calculations.

	B3LYP*	OPBE	TPSSh
LS-Co^{III}(Cat)(Sq)	0	0	0
S = 5/2	2.8	9.7	9.2

Table S6. Cartesian Coordinates of the optimized structure of **1** in the LS-Co^{III}(Cat)(Sq) state.

Atomic number	Element	Coordinates		
		X	Y	Z

1	Co	0	0	0
2	O	0	1.893311	0
3	O	-1.879068	0.121488	0.156435
4	N	0.151523	0.012425	1.968077
5	C	0.350595	0.436181	9.096387
6	C	0.370639	0.548882	10.587136
7	C	0.30391	0.256012	6.251141
8	C	-0.753213	-0.633949	2.718355
9	H	-1.520058	-1.181636	2.168914
10	C	-1.221721	2.37038	0.143877
11	C	0.269762	0.154346	4.771405
12	C	-0.723288	-0.590753	4.107694
13	H	-1.472713	-1.152698	4.666803
14	C	-2.261506	1.381841	0.233005
15	C	-3.605159	1.763019	0.404581
16	H	-4.345068	0.965647	0.472075
17	C	-1.549252	3.756161	0.219144
18	C	1.126606	0.708704	2.571261
19	H	1.839113	1.198685	1.906114
20	C	-0.88253	0.186145	7.006526
21	H	-1.844908	0.09131	6.498979
22	C	1.215956	0.803589	3.956325
23	H	2.008336	1.414923	4.39066
24	C	-0.859253	0.272827	8.396289
25	H	-1.797414	0.226332	8.952754
26	C	-2.899749	4.073823	0.392248
27	H	-3.174997	5.125134	0.459734
28	C	-3.942277	3.113157	0.494423
29	C	1.513158	0.438931	6.949905
30	H	2.456897	0.480989	6.401355
31	C	-0.450849	4.834494	0.120713
32	C	-5.389023	3.592518	0.727658
33	C	1.534078	0.53831	8.340106

34	H	2.488754	0.677642	8.853432
35	C	0.273471	4.717892	-1.241986
36	H	0.727976	3.725571	-1.3643
37	H	1.071048	5.476819	-1.31817
38	H	-0.431324	4.883058	-2.073797
39	C	-6.391362	2.424132	0.755904
40	H	-6.39167	1.861953	-0.191292
41	H	-7.411586	2.809463	0.914912
42	H	-6.174099	1.716303	1.571155
43	C	-5.815705	4.561097	-0.400306
44	H	-5.169563	5.450902	-0.448161
45	H	-6.849645	4.910209	-0.238284
46	H	-5.774105	4.064501	-1.383229
47	C	0.57121	4.643441	1.267072
48	H	0.077265	4.731029	2.248983
49	H	1.357241	5.416017	1.212378
50	H	1.050181	3.657404	1.207104
51	C	-1.021532	6.2608	0.231074
52	H	-1.741561	6.483042	-0.572586
53	H	-0.201338	6.992314	0.149756
54	H	-1.522058	6.433178	1.197318
55	C	-5.468492	4.325136	2.088726
56	H	-5.175189	3.653877	2.912153
57	H	-6.496933	4.67519	2.282255
58	H	-4.804099	5.202484	2.120944
59	N	-3.157686	-7.953027	8.361548
60	C	-0.7539	-1.676343	10.867957
61	C	-0.256764	-0.367975	11.392294
62	C	-1.702649	-4.184151	9.893082
63	C	-2.307504	-7.196454	7.662258
64	H	-2.007388	-7.578066	6.678577
65	C	-2.200548	-5.482266	9.370566
66	C	-1.805859	-5.972739	8.1126

67	H	-1.132771	-5.397037	7.473364
68	C	-3.535508	-7.494352	9.557869
69	H	-4.229207	-8.125249	10.127298
70	C	-0.399902	-3.73508	9.605292
71	H	0.273371	-4.366206	9.020433
72	C	-3.094505	-6.285224	10.101567
73	H	-3.429676	-5.987011	11.09742
74	C	0.063507	-2.51054	10.081697
75	H	1.083796	-2.198156	9.850703
76	C	-2.514183	-3.359335	10.695417
77	H	-3.537346	-3.666171	10.925249
78	C	-2.04707	-2.138767	11.180131
79	H	-2.703879	-1.521463	11.798054
80	N	-1.806359	0.878368	19.829661
81	C	-0.499156	-0.135836	12.848048
82	C	-1.026722	0.264171	15.623734
83	C	-0.764428	0.154958	19.410993
84	H	-0.116775	-0.266851	20.189563
85	C	-1.29712	0.473901	17.069444
86	C	-0.468507	-0.074758	18.065026
87	H	0.416929	-0.656261	17.798421
88	C	-2.598533	1.401499	18.889991
89	H	-3.455432	1.988379	19.243461
90	C	-0.468385	-0.939811	15.15361
91	H	-0.248736	-1.745775	15.857732
92	C	-2.393184	1.232877	17.518284
93	H	-3.098119	1.672514	16.809185
94	C	-0.223358	-1.140163	13.796228
95	H	0.192028	-2.094311	13.462705
96	C	-1.324929	1.25896	14.673107
97	H	-1.750171	2.210651	15.000534
98	C	-1.063515	1.065374	13.317996
99	H	-1.303356	1.859288	12.607896

100	N	4.763061	7.407886	13.548386
101	C	1.113224	1.729461	11.120641
102	C	2.5682	3.986612	12.084037
103	C	3.504005	7.519174	13.116355
104	H	3.058103	8.520644	13.160274
105	C	3.323536	5.162133	12.588264
106	C	2.750813	6.446055	12.633392
107	H	1.717511	6.608935	12.318892
108	C	5.31332	6.191422	13.508973
109	H	6.349266	6.111063	13.860959
110	C	1.642965	4.111782	11.030214
111	H	1.489484	5.084678	10.55716
112	C	4.648907	5.052574	13.046589
113	H	5.172644	4.094208	13.022242
114	C	0.942109	3.006463	10.550906
115	H	0.246043	3.134966	9.718234
116	C	2.758459	2.705681	12.63617
117	H	3.461856	2.571457	13.461366
118	C	2.045528	1.603657	12.168413
119	H	2.215437	0.624623	12.620711
120	O	0.000267	-1.893873	-0.000165
121	O	1.879496	-0.122106	-0.156537
122	C	1.221646	-2.370865	-0.145361
123	C	2.261602	-1.382285	-0.234461
124	C	3.605079	-1.763566	-0.407739
125	H	4.345055	-0.966257	-0.47517
126	C	1.548961	-3.756689	-0.222257
127	C	2.899223	-4.074299	-0.396724
128	H	3.17429	-5.125568	-0.465571
129	C	3.941856	-3.113629	-0.49904
130	C	0.450455	-4.834972	-0.124527
131	C	5.388245	-3.593102	-0.734158
132	C	-0.273508	-4.71951	1.238462

133	H	-0.727745	-3.727202	1.361884
134	H	-1.071263	-5.478303	1.314062
135	H	0.431418	-4.885705	2.069955
136	C	6.390775	-2.424896	-0.762776
137	H	6.392262	-1.863306	0.184766
138	H	7.410742	-2.810337	-0.923141
139	H	6.172758	-1.716524	-1.577354
140	C	5.815923	-4.562479	0.392754
141	H	5.169667	-5.452195	0.44072
142	H	6.849629	-4.911673	0.229431
143	H	5.775447	-4.066492	1.376029
144	C	-0.571881	-4.642869	-1.270473
145	H	-0.078193	-4.729606	-2.252587
146	H	-1.357884	-5.415501	-1.216257
147	H	-1.050853	-3.6569	-1.209519
148	C	1.020988	-6.261227	-0.23626
149	H	1.74119	-6.484248	0.56703
150	H	0.200746	-6.992733	-0.155385
151	H	1.521267	-6.432802	-1.202777
152	C	5.466062	-4.324871	-2.095777
153	H	5.172042	-3.653018	-2.918465
154	H	6.494216	-4.675024	-2.290617
155	H	4.801456	-5.202062	-2.127863
156	N	-0.151492	-0.012942	-1.968017
157	C	-0.351363	-0.43725	-9.096291
158	C	-0.371707	-0.549229	-10.58707
159	C	-0.304326	-0.25686	-6.251086
160	C	0.752559	0.634147	-2.718505
161	H	1.518859	1.182815	-2.169267
162	C	-0.269975	-0.155223	-4.77135
163	C	0.722401	0.590926	-4.10783
164	H	1.47113	1.153668	-4.667076
165	C	-1.125839	-0.710422	-2.571019

166	H	-1.837838	-1.200919	-1.905719
167	C	0.881742	-0.184363	-7.006793
168	H	1.844068	-0.087732	-6.499482
169	C	-1.215257	-0.805548	-3.956067
170	H	-2.006992	-1.41785	-4.390194
171	C	0.858295	-0.271235	-8.396542
172	H	1.796075	-0.221301	-8.953386
173	C	-1.513459	-0.441698	-6.949569
174	H	-2.45699	-0.485384	-6.400805
175	C	-1.534543	-0.54112	-8.339766
176	H	-2.489179	-0.681422	-8.852909
177	N	3.140182	7.958164	-8.35662
178	C	0.748024	1.678454	-10.866522
179	C	0.2532	0.369586	-11.391822
180	C	1.692128	4.187372	-9.890061
181	C	2.292163	7.199207	-7.657286
182	H	1.992041	7.579359	-6.673041
183	C	2.18756	5.486189	-9.366917
184	C	1.792822	5.974767	-8.108225
185	H	1.121512	5.397052	-7.46894
186	C	3.518052	7.501282	-9.553613
187	H	4.210025	8.134093	-10.123018
188	C	0.390667	3.73513	-9.601467
189	H	-0.283364	4.364106	-9.015168
190	C	3.079239	6.291644	-10.097955
191	H	3.414305	5.994905	-11.094286
192	C	-0.070367	2.509894	-10.078391
193	H	-1.089752	2.195034	-9.846756
194	C	2.5047	3.365206	-10.69408
195	H	3.526871	3.674691	-10.924776
196	C	2.039826	2.144094	-11.179588
197	H	2.697514	1.5287	-11.798479
198	N	1.803662	-0.865516	-19.830758

199	C	0.495486	0.139104	-12.847874
200	C	1.022866	-0.257362	-15.62412
201	C	0.760292	-0.144636	-19.411291
202	H	0.111761	0.276698	-20.18939
203	C	1.293571	-0.465122	-17.070065
204	C	0.463897	0.082991	-18.06507
205	H	-0.422646	0.662543	-17.797896
206	C	2.596865	-1.38809	-18.891653
207	H	3.454902	-1.972929	-19.245745
208	C	0.461994	0.944961	-15.152743
209	H	0.240744	1.751248	-15.855991
210	C	2.391164	-1.221386	-17.519764
211	H	3.097038	-1.660359	-16.811188
212	C	0.21726	1.143699	-13.795066
213	H	-0.200273	2.096577	-13.46059
214	C	1.323106	-1.252501	-14.674504
215	H	1.750084	-2.203084	-15.002888
216	C	1.061738	-1.060676	-13.319127
217	H	1.303396	-1.854761	-12.609819
218	N	-4.748682	-7.417843	-13.548916
219	C	-1.111537	-1.731407	-11.120909
220	C	-2.561047	-3.991842	-12.084761
221	C	-3.489113	-7.526304	-13.117643
222	H	-3.040897	-8.526717	-13.162082
223	C	-3.31389	-5.168991	-12.588949
224	C	-2.738158	-6.451551	-12.634824
225	H	-1.704275	-6.612072	-12.321042
226	C	-5.301726	-6.202668	-13.508942
227	H	-6.338057	-6.124632	-13.860318
228	C	-1.634996	-4.115146	-11.031422
229	H	-1.478903	-5.087838	-10.55882
230	C	-4.639726	-5.062394	-13.046611
231	H	-5.165639	-4.10523	-13.021874

232	C	-0.936666	-3.008276	-10.552011
233	H	-0.239687	-3.135397	-9.719887
234	C	-2.755152	-2.711077	-12.635923
235	H	-3.459585	-2.578205	-13.460454
236	C	-2.044735	-1.607459	-12.168074
237	H	-2.217317	-0.628661	-12.619876

Table S7. Cartesian Coordinates of the optimized structure of **1** in the HS-$Co^{II}(Sq)_2$ state.

Atomic number	Element	Coordinates		
		X	Y	Z
1	Co	0	0	0
2	O	0	2.083541	0
3	O	-2.030616	0.394366	-0.11318
4	N	-0.069626	0.085028	2.210013
5	C	-0.540434	0.859187	9.312192
6	C	-0.650961	1.037881	10.792743
7	C	-0.334028	0.550665	6.483767
8	C	-1.141407	-0.351715	2.885824
9	H	-1.935659	-0.805555	2.28653
10	C	-1.173722	2.593372	-0.034923
11	C	-0.23397	0.379125	5.012206
12	C	-1.25949	-0.234885	4.268667
13	H	-2.147061	-0.637105	4.759854
14	C	-2.304382	1.6472	-0.084352
15	C	-3.638571	2.143419	-0.095194
16	H	-4.433287	1.398159	-0.125564
17	C	-1.442955	4.013557	-0.015866
18	C	0.927848	0.654413	2.901049
19	H	1.787842	0.985887	2.313212
20	C	-1.586409	0.667153	7.116886
21	H	-2.499772	0.668457	6.518251
22	C	0.88436	0.825174	4.283048

23	H	1.714125	1.331127	4.779487
24	C	-1.687348	0.813581	8.498579
25	H	-2.673371	0.907165	8.958393
26	C	-2.771029	4.405662	-0.026668
27	H	-2.995102	5.471114	-0.004642
28	C	-3.888568	3.502751	-0.060325
29	C	0.814424	0.612883	7.297364
30	H	1.804683	0.509414	6.848275
31	C	-0.277922	5.022174	0.024903
32	C	-5.312608	4.088558	-0.031511
33	C	0.713648	0.777346	8.677776
34	H	1.624187	0.821219	9.280748
35	C	0.612931	4.839126	-1.227848
36	H	1.019286	3.820421	-1.280132
37	H	1.456788	5.549576	-1.201389
38	H	0.036964	5.033595	-2.147978
39	C	-6.39277	2.996043	-0.127304
40	H	-6.308034	2.417935	-1.060862
41	H	-7.393268	3.457514	-0.110384
42	H	-6.33886	2.29017	0.716167
43	C	-5.508177	5.06163	-1.2183
44	H	-4.798786	5.902704	-1.188875
45	H	-6.525848	5.486497	-1.200808
46	H	-5.373008	4.542642	-2.18099
47	C	0.566843	4.791209	1.301833
48	H	-0.0493	4.923983	2.206726
49	H	1.395247	5.518629	1.346524
50	H	0.991233	3.779095	1.316796
51	C	-0.772213	6.48069	0.043065
52	H	-1.364301	6.730082	-0.852078
53	H	0.093808	7.161604	0.064115
54	H	-1.384668	6.700275	0.932405
55	C	-5.517053	4.853145	1.298981

56	H	-5.391827	4.178932	2.161613
57	H	-6.532282	5.282259	1.34477
58	H	-4.799516	5.680299	1.413969
59	N	-4.770339	-7.189083	8.544097
60	C	-2.013927	-1.053499	11.038121
61	C	-1.440749	0.223121	11.563381
62	C	-3.107875	-3.503372	10.067388
63	C	-3.789627	-6.547562	7.90305
64	H	-3.437106	-7.000683	6.968305
65	C	-3.678262	-4.772484	9.54779
66	C	-3.216886	-5.355568	8.353601
67	H	-2.434719	-4.874801	7.761853
68	C	-5.212417	-6.641968	9.679703
69	H	-6.013853	-7.178852	10.202164
70	C	-1.746858	-3.190962	9.889828
71	H	-1.086843	-3.907767	9.39563
72	C	-4.709825	-5.454578	10.217846
73	H	-5.106193	-5.080567	11.164418
74	C	-1.212694	-1.994877	10.364187
75	H	-0.149991	-1.790154	10.221275
76	C	-3.906208	-2.570576	10.756682
77	H	-4.971197	-2.769887	10.897834
78	C	-3.369455	-1.378221	11.239697
79	H	-4.017739	-0.674676	11.767925
80	N	-3.63841	1.991038	19.76035
81	C	-1.794795	0.542199	12.979351
82	C	-2.53562	1.115848	15.674651
83	C	-2.635686	1.157293	19.471019
84	H	-2.105754	0.714425	20.323425
85	C	-2.916993	1.415679	17.078855
86	C	-2.239802	0.840104	18.169237
87	H	-1.392839	0.168739	18.010676
88	C	-4.286914	2.540659	18.730034

89	H	-5.113095	3.218805	18.977399
90	C	-2.056157	-0.155272	15.304899
91	H	-1.982052	-0.945203	16.056
92	C	-3.972587	2.291342	17.391683
93	H	-4.563777	2.760495	16.602113
94	C	-1.707161	-0.439281	13.985694
95	H	-1.35779	-1.442326	13.728702
96	C	-2.647098	2.089499	14.66386
97	H	-3.006317	3.090632	14.913781
98	C	-2.281184	1.810813	13.348321
99	H	-2.376377	2.590141	12.589578
100	N	4.093083	7.583825	13.915021
101	C	0.151177	2.165911	11.352724
102	C	1.723367	4.318391	12.369804
103	C	2.898498	7.792304	13.354854
104	H	2.551046	8.832233	13.315598
105	C	2.538734	5.440158	12.902028
106	C	2.093421	6.772975	12.840165
107	H	1.116325	7.016964	12.417181
108	C	4.522298	6.320493	13.97754
109	H	5.506635	6.159958	14.434544
110	C	0.923169	4.479226	11.222622
111	H	0.915266	5.437701	10.698071
112	C	3.796647	5.228411	13.494874
113	H	4.223436	4.22491	13.559615
114	C	0.165915	3.423532	10.718053
115	H	-0.428634	3.57627	9.813924
116	C	1.729472	3.054054	12.988871
117	H	2.331786	2.894248	13.886344
118	C	0.958829	2.003545	12.494789
119	H	0.983976	1.036618	13.001095
120	O	0.000548	-2.083931	0.000125
121	O	2.030722	-0.394112	0.11291

122	C	1.174437	-2.593352	0.034175
123	C	2.304854	-1.646865	0.083649
124	C	3.639183	-2.142724	0.093862
125	H	4.433714	-1.397273	0.124448
126	C	1.444098	-4.013462	0.014026
127	C	2.772278	-4.405188	0.024083
128	H	2.996657	-5.47056	0.00133
129	C	3.88956	-3.501972	0.05802
130	C	0.279342	-5.022378	-0.027034
131	C	5.313747	-4.087377	0.028245
132	C	-0.611197	-4.840447	1.226099
133	H	-1.017831	-3.821894	1.27919
134	H	-1.454859	-5.551118	1.199397
135	H	-0.034904	-5.035385	2.145928
136	C	6.393666	-2.994679	0.124664
137	H	6.309076	-2.417413	1.058754
138	H	7.394273	-3.455889	0.107026
139	H	6.339327	-2.288079	-0.718172
140	C	5.509949	-5.06147	1.214091
141	H	4.800761	-5.902695	1.184136
142	H	6.52772	-5.486065	1.195881
143	H	5.374966	-4.543384	2.177291
144	C	-0.565834	-4.790794	-1.303588
145	H	0.050071	-4.922998	-2.208727
146	H	-1.394144	-5.518312	-1.348452
147	H	-0.990371	-3.778728	-1.317903
148	C	0.774049	-6.480739	-0.046307
149	H	1.36653	-6.730547	0.848462
150	H	-0.091783	-7.16189	-0.067502
151	H	1.386251	-6.69957	-0.936006
152	C	5.517963	-4.850723	-1.303001
153	H	5.392252	-4.175778	-2.164992
154	H	6.5333	-5.279503	-1.349518

155	H	4.800627	-5.677982	-1.418489
156	N	0.07002	-0.085112	-2.209987
157	C	0.543965	-0.85577	-9.312159
158	C	0.654965	-1.034579	-10.79256
159	C	0.336428	-0.548456	-6.483765
160	C	1.145282	0.345657	-2.884186
161	H	1.941535	0.79411	-2.283508
162	C	0.235841	-0.377902	-5.012169
163	C	1.264277	0.229151	-4.266974
164	H	2.154776	0.626443	-4.7569
165	C	-0.930037	-0.647966	-2.902625
166	H	-1.792702	-0.974634	-2.315982
167	C	1.588673	-0.674215	-7.115362
168	H	2.501199	-0.683443	-6.515499
169	C	-0.885979	-0.817863	-4.284724
170	H	-1.718151	-1.318441	-4.782618
171	C	1.690192	-0.820174	-8.497061
172	H	2.67602	-0.921101	-8.955757
173	C	-0.811461	-0.600577	-7.298835
174	H	-1.801413	-0.489669	-6.850813
175	C	-0.710234	-0.764286	-8.679291
176	H	-1.620334	-0.80082	-9.283411
177	N	4.834488	7.15735	-8.530731
178	C	2.035096	1.045519	-11.034989
179	C	1.45235	-0.22603	-11.56187
180	C	3.146117	3.486429	-10.061158
181	C	3.850895	6.520223	-7.889717
182	H	3.502841	6.972975	-6.953122
183	C	3.725409	4.750551	-9.539249
184	C	3.269811	5.333159	-8.342609
185	H	2.485883	4.855478	-7.750678
186	C	5.271172	6.610607	-9.668602
187	H	6.074981	7.143973	-10.191022

188	C	1.783249	3.182739	-9.882792
189	H	1.128539	3.902904	-9.386421
190	C	4.760175	5.42791	-10.209175
191	H	5.15272	5.053897	-11.157342
192	C	1.240757	1.991047	-10.358728
193	H	0.176883	1.793008	-10.214947
194	C	3.937474	2.549883	-10.753431
195	H	5.003602	2.742465	-10.895368
196	C	3.392449	1.36178	-11.237723
197	H	4.035456	0.655129	-11.768262
198	N	3.658223	-2.016532	-19.751794
199	C	1.806745	-0.548645	-12.976908
200	C	2.549497	-1.130548	-15.670004
201	C	2.664562	-1.1708	-19.465989
202	H	2.143806	-0.720693	-20.320248
203	C	2.93252	-1.434484	-17.072876
204	C	2.266956	-0.849935	-18.165637
205	H	1.427625	-0.168369	-18.010127
206	C	4.295469	-2.575006	-18.719234
207	H	5.114261	-3.263096	-18.963679
208	C	2.081858	0.145458	-15.301876
209	H	2.018258	0.93601	-16.053275
210	C	3.978568	-2.322846	-17.38203
211	H	4.56082	-2.79964	-16.590421
212	C	1.732068	0.433417	-13.983728
213	H	1.392146	1.440029	-13.728012
214	C	2.647684	-2.105112	-14.65872
215	H	2.997253	-3.109973	-14.907293
216	C	2.281082	-1.822285	-13.34431
217	H	2.366154	-2.602358	-12.585151
218	N	-4.149487	-7.530166	-13.926853
219	C	-0.157142	-2.154472	-11.354532
220	C	-1.749313	-4.2902	-12.375407

221	C	-2.954216	-7.750339	-13.37265
222	H	-2.614434	-8.793024	-13.339937
223	C	-2.575188	-5.403269	-12.909599
224	C	-2.139517	-6.739609	-12.856128
225	H	-1.162426	-6.992841	-12.438588
226	C	-4.569481	-6.263382	-13.981513
227	H	-5.554494	-6.09329	-14.433578
228	C	-0.948169	-4.461616	-11.230414
229	H	-0.947089	-5.421969	-10.709226
230	C	-3.833743	-5.179145	-13.496458
231	H	-4.253063	-4.172105	-13.554797
232	C	-0.181108	-3.41396	-10.723913
233	H	0.413783	-3.574526	-9.821354
234	C	-1.746632	-3.023669	-12.989956
235	H	-2.34967	-2.85581	-13.885483
236	C	-0.965888	-1.981415	-12.494208
237	H	-0.984045	-1.01251	-12.997056

4. Additional Figures

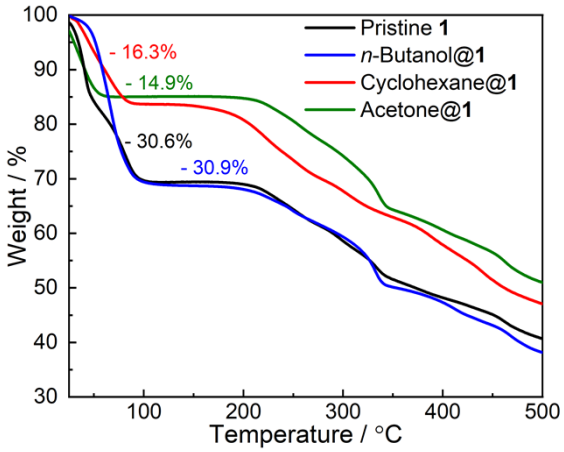

Fig. S1 Thermogravimetric analysis of **1** and other samples loaded with different solvent molecules. Solvent molecules are calculated based on thermogravimetric analysis : Pristine **1** (six methanol and two toluene molecules); *n*-Butanol@**1** (five *n*-butanol molecules); Cyclohexane@**1** (two cyclohexane molecules); Acetone@**1** (two and half acetone molecules)

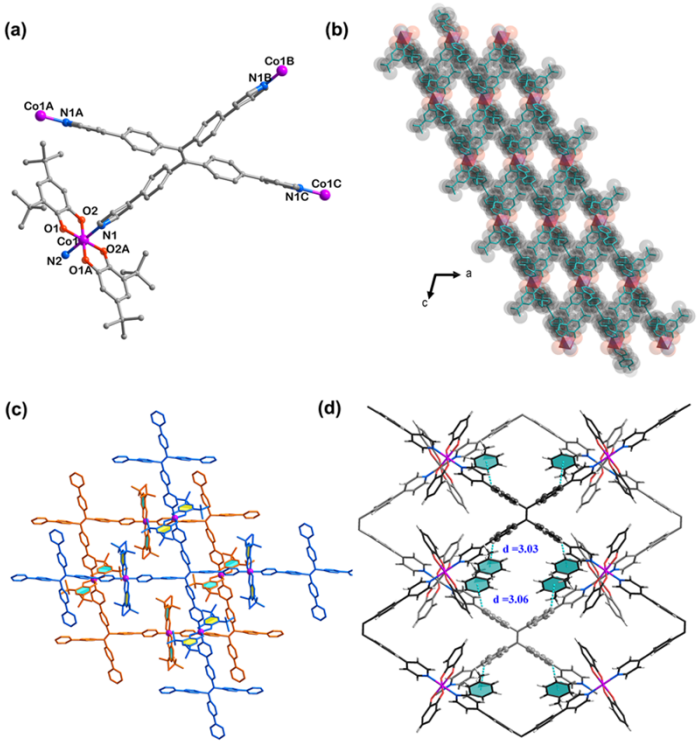

Fig. S2 Crystal structure of **1**. (a) Coordination environment around the Co^{II} center. (b) Viewed along the *b* axis showing rhombic pores, hydrogen atoms are removed for clarity. (c) Interdigitation of adjacent layers

in ABAB type stacking (two layers are shown in different colors). (d) Intermolecular interactions of C–H···π. *tert*-Butyl groups are removed for clarity.

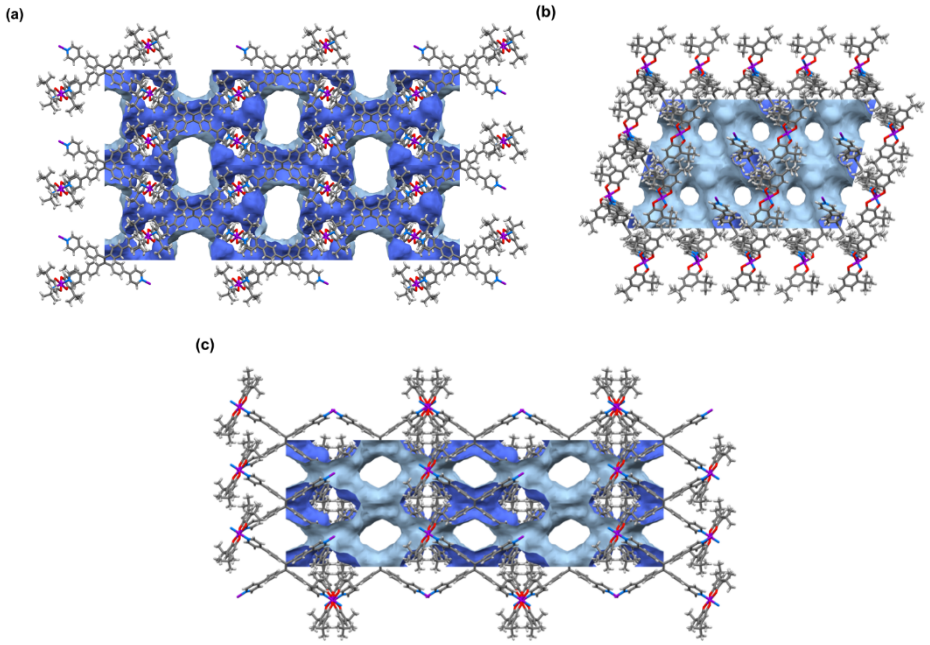

Fig. S3 Voids in the framework of **1** viewed along the crystallographic *a* (top panel), *b* (middle panel) and *c* (bottom panel) axes.

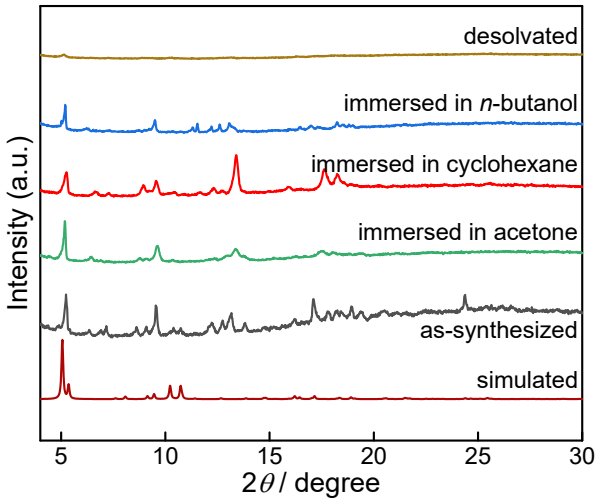

Fig. S4 Powder X-ray diffraction patterns for **1** and other samples loaded with different solvent molecules. For fresh sample of **1**, the slight peak shifts might be due to the interlayer slipping caused by partial loss of solvent molecules under atmosphere. As for solvent exchanged samples, the slightly different PXRD patterns may indicate certain degree of structural rearrangement induced by guest

solvents. The desolvated sample is essentially featureless, which indicates complete loss of sample crystallinity.

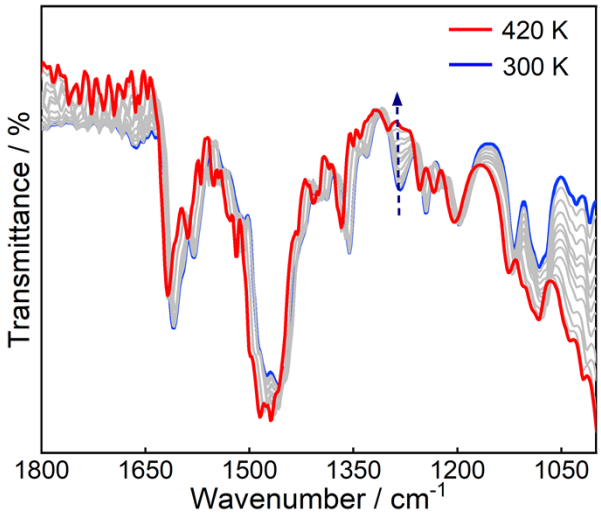

Fig. S5 Temperature-dependent IR spectra of **1**. Upon temperature increasing, a slightly left shift of the IR spectra might be due to solvent loss. Infrared spectrum of **1** at room temperature exhibits a strong band at 1595 cm^{-1}, which can be ascribed to the pyridine C–N stretches of TPPE, and the band at ca. 1283 cm^{-1} of intermediate intensity is assigned to the catecholate C–O stretching.[9] The strong bands observed at 1400-1600 cm^{-1} are assigned to TPPE bond stretches, which obscure the characteristic semiquinone C=O stretching band of relatively weak intensity.[10]

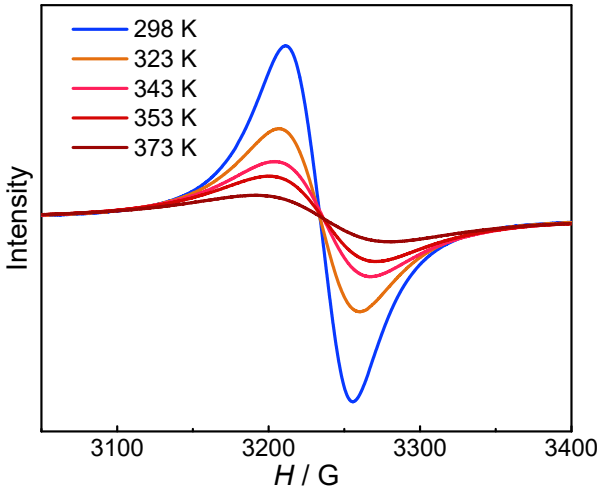

Fig. S6 Variable-temperature EPR spectra of **1**. The X-band solid-state EPR spectrum of **1** at 300 K reveals a relatively isotropic EPR signal at g = 1.999 with no resolved hyperfine features, which can be assigned to the ligand-based radical LS-Co^{III}(Cat)(Sq).[11] Upon warming up, the signal intensity

decreases drastically and becomes barely observable at 400 K. This can be rationalized by the fact that higher temperature increases the population of HS-$Co^{II}(Sq)_2$ tautomer which is usually EPR silent due to extensive hyperfine interactions involving the paramagnetic HS-Co^{II} ion and spin delocalization through metal-ligand covalency and/or spin-polarization effects, together with the rapid electronic relaxation of HS-Co^{II} ion arising from spin-orbit coupling resulting in rapid spin-relaxation faster than the EPR timescale.[12]

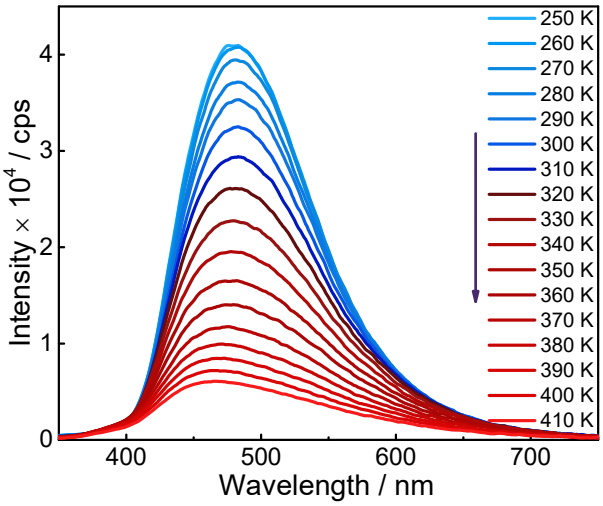

Fig. S7 Temperature-dependent emission spectra of **1** at λ_{ex} = 320 nm.

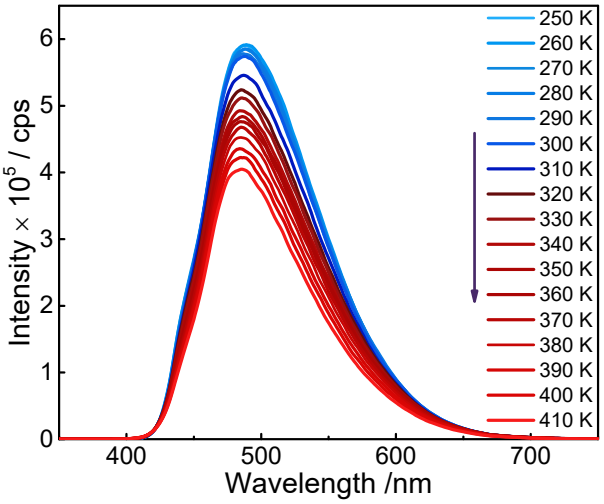

Fig. S8 Temperature-dependent emission spectra of TPPE at λ_{ex} = 320 nm.

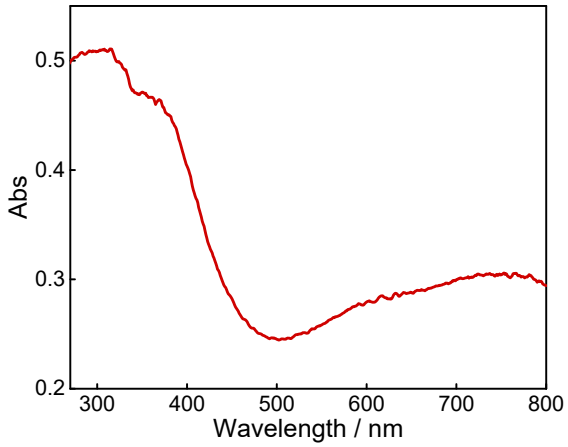

Fig. S9 Solid-state UV-vis absorption spectra of **1** at the room temperature.

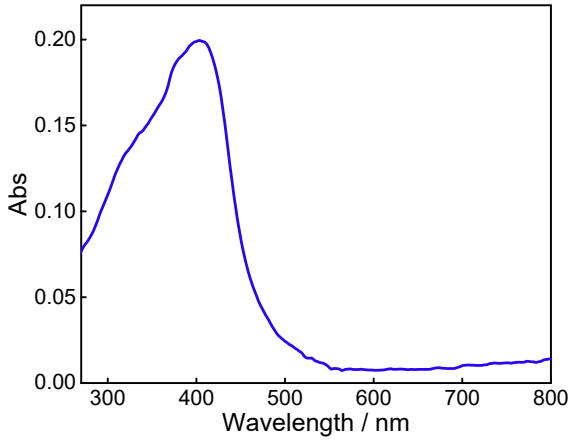

Fig. S10 Solid-state UV-vis absorption spectra of TPPE at the room temperature.

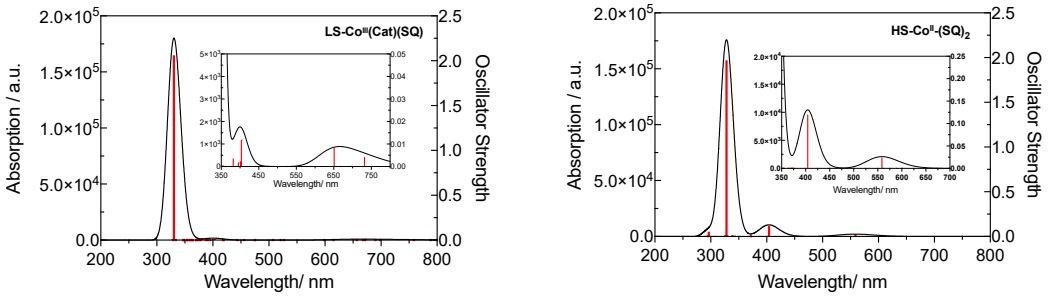

Fig. S11 Electronic absorption spectra of **1** calculated for the LS-Co^{III}(Cat)(Sq) and HS-$Co^{II}(Sq)_2$ tautomers (between 200 and 800 nm) with CAM-B3LYP.

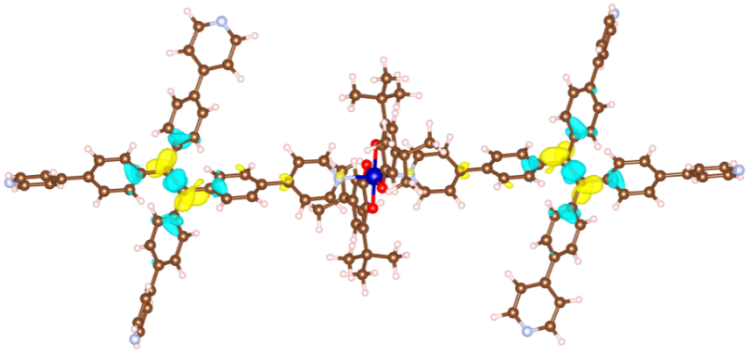

Fig. S12 Difference density map between excited and ground states of **1** LS-Co^{III}(Cat)(Sq) tautomeric form for the absorption at 331 nm. Yellow indicates increase of electron density, whereas cyan indicates loss of electron density. Isovalue = 0.001 a.u.

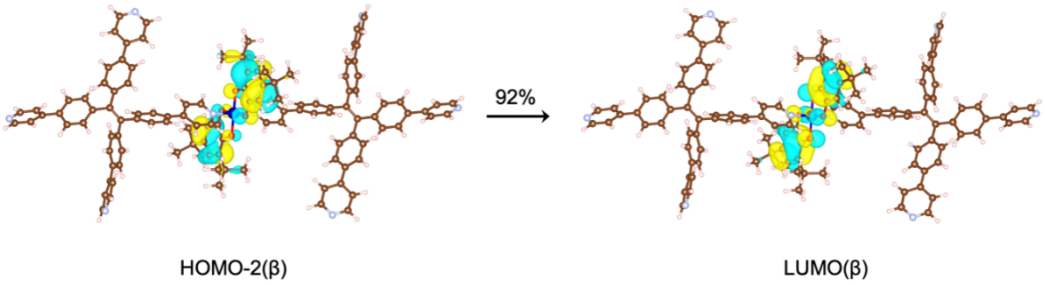

Fig. S13 Dominant molecule-orbital contributions for the 651 nm transition for the LS-Co^{III}(Cat)(Sq) tautomeric form of **1**, corresponding to a $Sq^{\bullet-}$ $\pi \rightarrow \pi^*$ transition. Isovalue = 0.025 a.u.

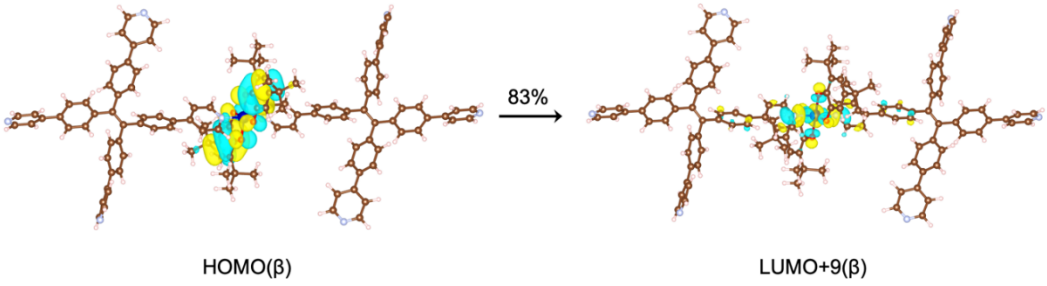

Fig. S14 Dominant molecule-orbital contributions for the 732 nm transition for the LS-Co^{III}(Cat)(Sq) tautomeric form of **1**, corresponding to a LMCT ($Cat^{2-} \rightarrow$ LS-Co^{III} e_g*) transition. Isovalue = 0.025 a.u.

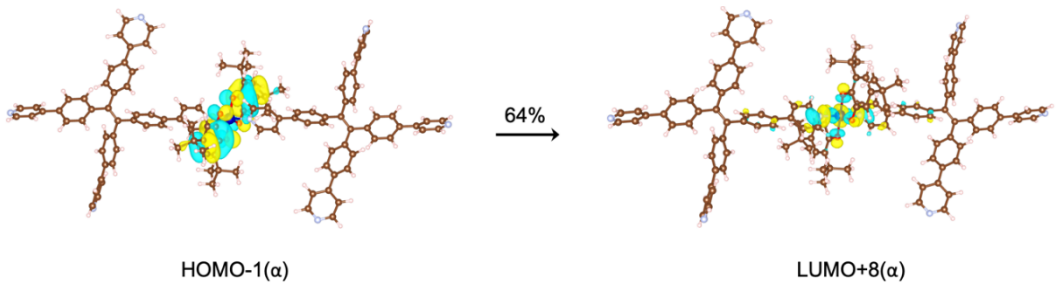

Fig. S15 Dominant molecular-orbital contributions for the 404 nm transition for the LS-Co^{III}(Cat)(Sq) tautomeric form of **1**, corresponding to a LMCT (Cat^{2-} → LS-Co^{III} e_g*) transition. Isovalue = 0.025 a.u.

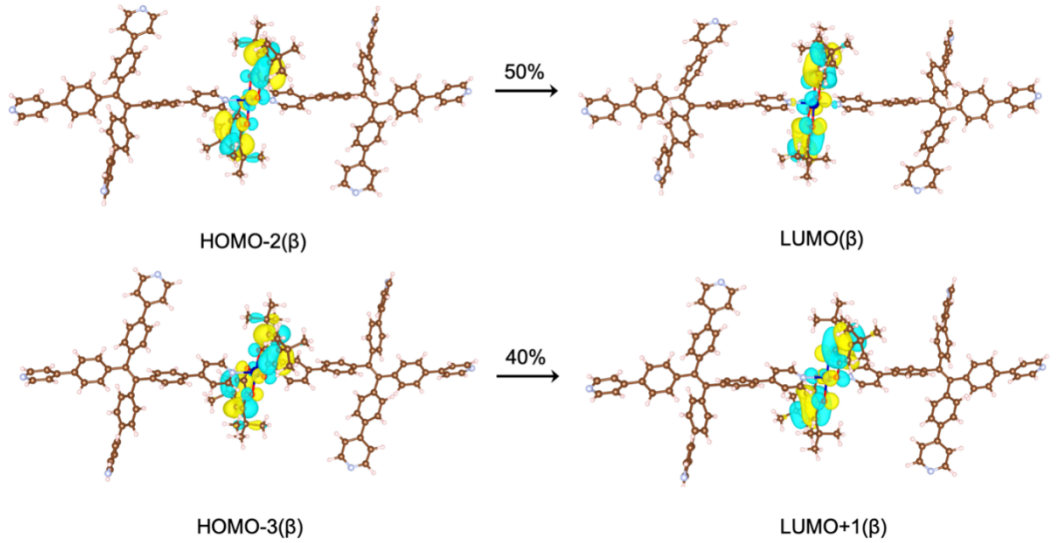

Fig. S16 Dominant molecular-orbital contributions for the 559 nm transition for the HS-$Co^{II}(Sq)_2$ tautomeric form of **1**, corresponding to $Sq^{\bullet-}$ π → π* transitions. Isovalue = 0.025 a.u.

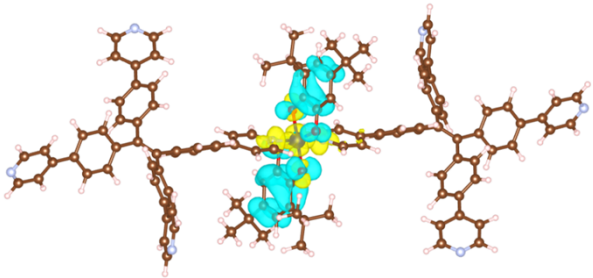

Fig. S17 Difference density map between excited and ground states of **1** LS-Co^{III}(Cat)(Sq) tautomeric form for the absorption at 404 nm. Yellow indicates increase of electron density, whereas cyan indicates loss of electron density. Isovalue = 0.001 a.u.

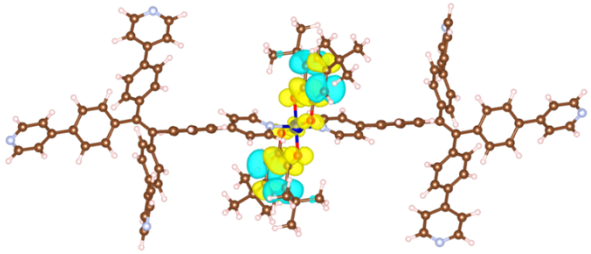

Fig. S18 Difference density map between excited and ground states of **1** LS-Co^{III}(Cat)(Sq) tautomeric form for the absorption at 651 nm. Yellow indicates increase of electron density, whereas cyan indicates loss of electron density. Isovalue = 0.001 a.u.

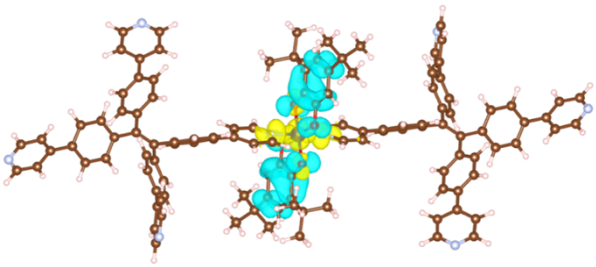

Fig. S19 Difference density map between excited and ground states of **1** LS-Co^{III}(Cat)(Sq) tautomeric form for the absorption at 732 nm. Yellow indicates increase of electron density, whereas cyan indicates loss of electron density. Isovalue = 0.001 a.u.

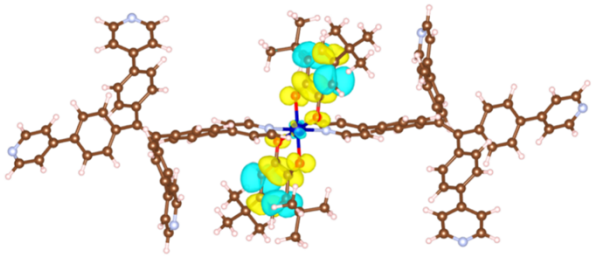

Fig. S20 Difference density map between excited and ground states of **1** HS-$Co^{II}(Sq)_2$ tautomeric form for the absorption at 559 nm. Yellow indicates increase of electron density, whereas cyan indicates loss of electron density. Isovalue = 0.001 a.u.

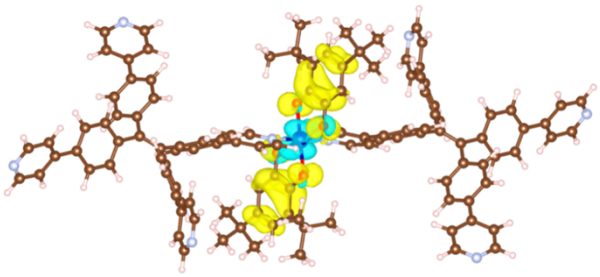

Fig. S21 Difference density map between excited and ground states of **1** HS-$Co^{II}(Sq)_2$ tautomeric form for the absorption at 404 nm. Yellow indicates increase of electron density, whereas cyan indicates loss of electron density. Isovalue = 0.001 a.u.

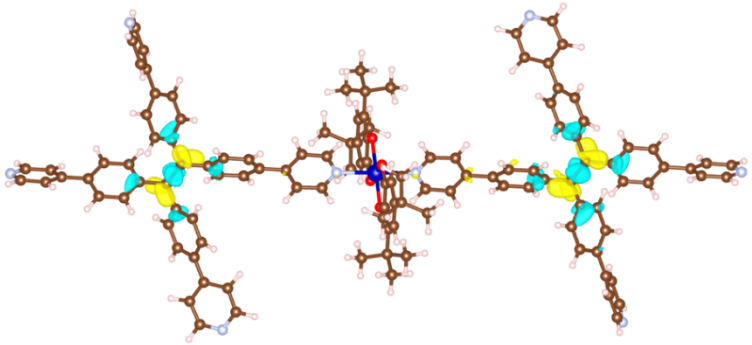

Fig. S22 Difference density map between excited and ground states of **1** HS-$Co^{II}(Sq)_2$ tautomeric form for the absorption at 328 nm. Yellow indicates increase of electron density, whereas cyan indicates loss of electron density. Isovalue = 0.001 a.u.

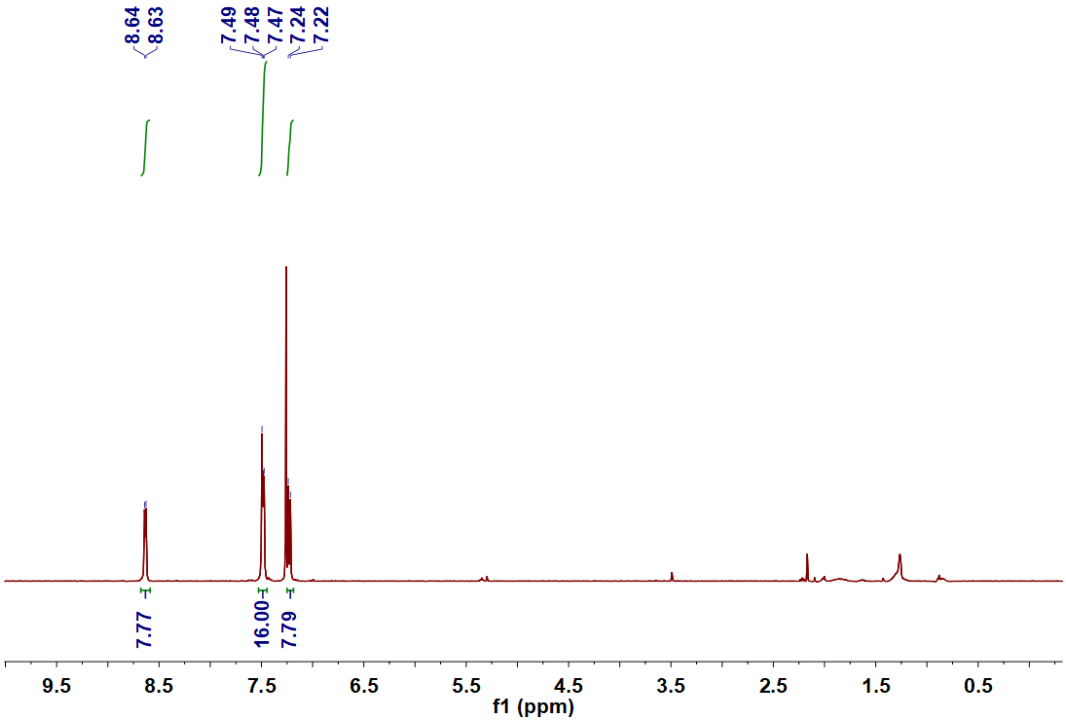

Fig. S23 ^{1}H NMR spectrum (400 MHz, $CDCl_3$, 298K) recorded for ligand TPPE.

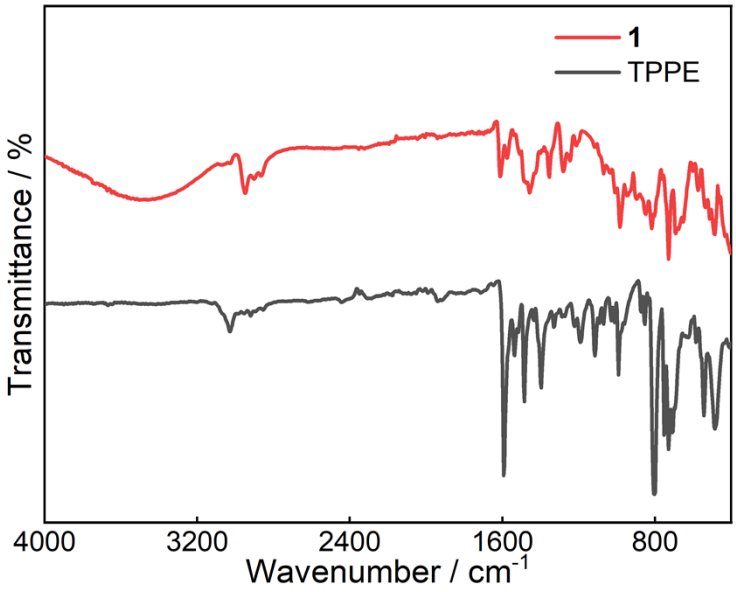

Fig. S24 IR spectra of **1** and TPPE at the room temperature.

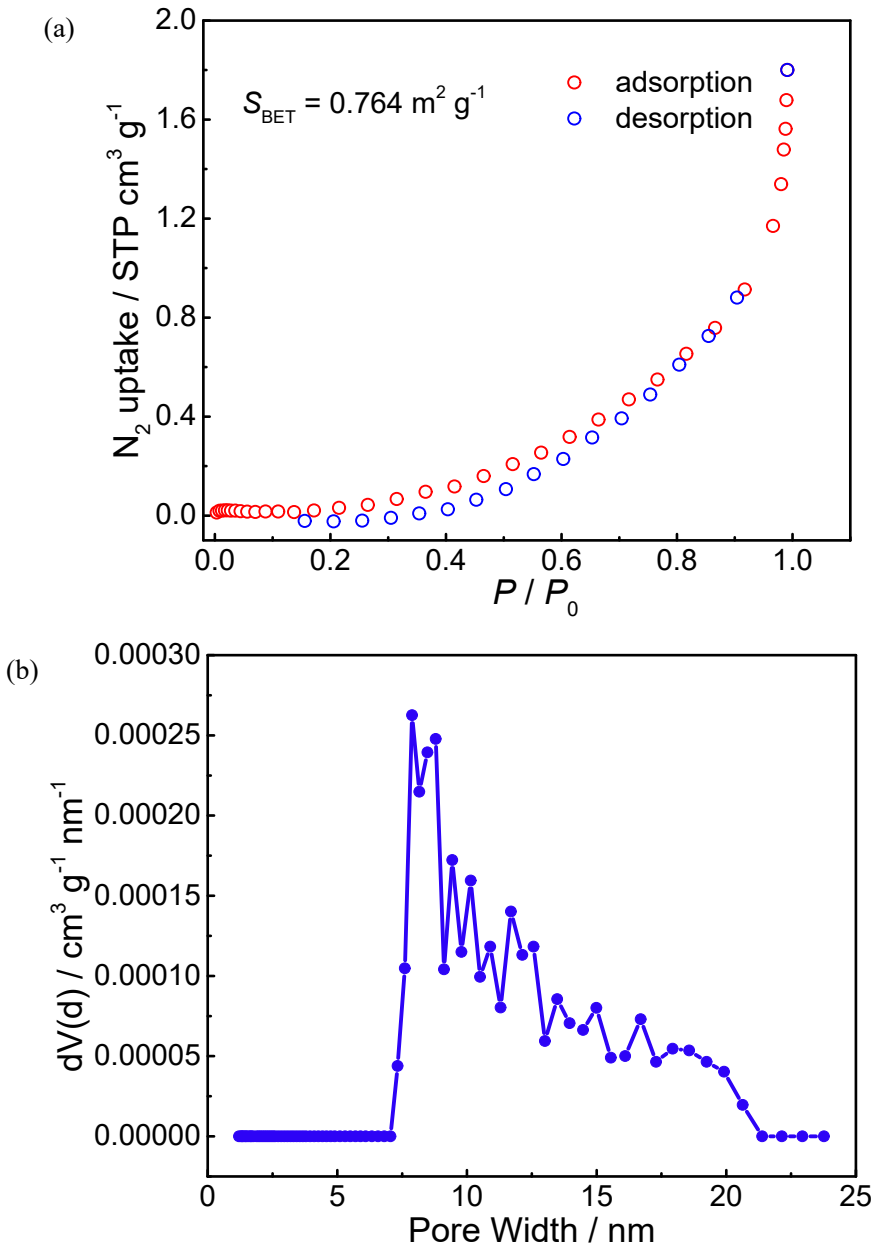

Fig. S25 (a) N_2 adsorption-desorption isotherms of **1**; (b) pore size distribution profiles of desolvated **1** at 77 K. According to TGA, **1** started to lose toluene molecules around 350 K, which coincides with the sudden increase of $\chi_M T$ at around 350 K. As shown in Fig. S2, the toluene molecules are tightly wrapped by tetraphenylene and dioxolene ligands between adjacent layers to support the ABAB stacking structure by acting as an "anchor", leading to small motional freedom around the cobalt–dioxolene units that hinders the expansion of cobalt coordination sphere for VT transition to occur.[13] The removal of toluene molecules may destabilize the stacked 2D structure through interlayer slipping, alleviating the constraints around cobalt–dioxolene moieties that facilitates VT transition.

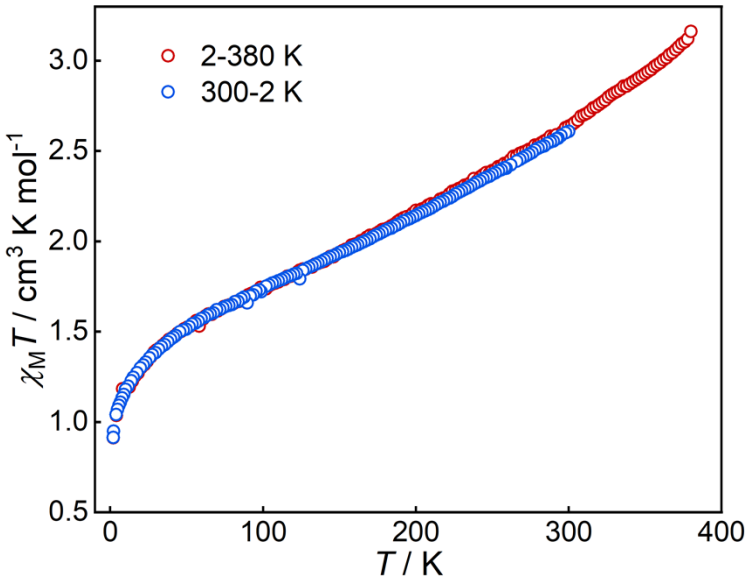

Fig. S26 $\chi_M T$ versus T plots for desolvated **1** under applied field of 5000 Oe. In view of the fact that the abrupt VT transition of the fresh sample at 350 K, variable-temperature dc magnetization measurements were carried out on the sample heated and evacuated at 80 ℃. It is obvious that a totally distinct magnetic behavior was observed. Upon cooling, the $\chi_M T$ value decreases gradually from 2.6 $cm^3\,K\,mol^{-1}$ at 300 K to 0.92 $cm^3\,K\,mol^{-1}$ at 2 K. During the heating process, the $\chi_M T$ value keeps growing until 3.15 $cm^3\,K\,mol^{-1}$ at 380 K, higher than the theoretical value, which might attribute to the orbital contribution of the HS-Co^{II}.

5. References

1. Sheldrick, G. M. Crystal structure refinement with SHELXL. Acta Cryst. C. 71, 3–8 (2015)
2. Dolomanov, O. V.; Bourhis, L. J.; Gildea, R. J.; Howard, J. A.K.; Puschmann, *J. Appl. Crystallogr.* 2009, **42**, 339−341.
3. F. Neese, *WIREs Comput. Mol. Sci.*, 2012, **2**, 73-78.
4. F. Neese, F. Wennmohs, A. Hansen and U. Becker, *Chem. Phys.*, 2009, **356**, 98-109.
5. a) K. Eichkorn, F. Weigend, O. Treutler and R. Ahlrichs, *Theor. Chem. Accounts*, 1997, **97**, 119-124; b) K. Eichkorn, O. Treutler, H. Öhm, M. Häser and R. Ahlrichs, *Chem. Phys. Lett.*, 1995, **242**, 652-660.

6. a) T. Soda, Y. Kitagawa, T. Onishi, Y. Takano, Y. Shigeta, H. Nagao, Y. Yoshioka and K. Yamaguchi, *Chem. Phys. Lett.*, 2000, **319**, 223-230; b) S. Grimme, J. Antony, S. Ehrlich and H. Krieg, *J. Chem. Phys.*, 2010, **132**, 154104.
7. Y. Matt, I. Wessely, L. Gramespacher, M. Tsotsalas and S. Bräse, *Eur. J. Org. Chem.*, 2021, **2021**, 239-245.
8. C. Mu, Z. Zhang, Y. Hou, H. Liu, L. Ma, X. Li, S. Ling, G. He and M. Zhang, *Angew. Chem. Int. Ed.*, 2021, **60**, 12293-12297.
9. E. Evangelio, D. N. Hendrickson and D. Ruiz-Molina, *Inorg. Chimica Acta*, 2008, **361**, 3403-3409.
10. A. Panja and A. Frontera, *Eur. J. Inorg. Chem.*, 2018, **2018**, 924-931.
11. D. M. Adams, A. Dei, A. L. Rheingold and D. N. Hendrickson, *J. Am. Chem. Soc.,* 1993, **115**, 8221-8229.
12. a) N. M. Bonanno, Z. Watts, C. Mauws, B. O. Patrick, C. R. Wiebe, Y. Shibano, K. Sugisaki, H. Matsuoka, D. Shiomi, K. Sato, T. Takui and M. T. Lemaire, *Chem. Commun. (Camb)*, 2021, **57**, 6213-6216; b) A. Witt, F. W. Heinemann and M. M. Khusniyarov, *Chem. Sci.*, 2015, **6**, 4599-4609.
13. E. Evangelio, C. Rodriguez-Blanco, Y. Coppel, D. N. Hendrickson, J. P. Sutter, J. Campo and D. Ruiz-Molina, *Solid State Sci.*, 2009, **11**, 793-800.